Enhanced adsorptive desulfurization by iso-structural amino bearing IRMOF-3 and IRMOF-3@Al_2O_3 versus MOF-5 and MOF-5@Al_2O_3 revealing the predominant role of hydrogen bonding

Zareen Zuhra[1], Cuncun Mu[1], Fang Tang, Yunshan Zhou*, Lijuan Zhang*, Zipeng Zhao and Libo Qin

State Key Laboratory of Chemical Resource Engineering, Institute of Science, Beijing University of Chemical Technology, Beijing 100029, P. R. China

1. Experimental

1.1. Materials

γ-Al_2O_3 beads (S_{BET}, 192.08 m^2 g^{-1}; V_{total}, 0.679 cm^3 g^{-1}; average pore size, 12.06 nm; diameter, ca.2 mm) were supplied by the State Key Laboratory of Chemical Resource Engineering (Beijing University of Chemical Technology, China), and were washed with distilled water and pre-treated at 200 °C for 2 hours in muffle furnace every time before use to remove water and other contaminants. All the other chemicals were purchased from commercial sources: zinc nitrate hexahydrate (AR grade) and *N*,*N*-dimethyl formamide (DMF, AR grade) were from Beijing Chemical Reagent Co. Ltd.; terephthalic acid (H_2BDC, 99%) was from Aladdin Reagent Co. Ltd.; 2-amion terephthalic acid was from Alfa Aesar Chemical Co. Ltd.; n-octane (AR grade) was from Tianjin Guangfu Technology Development Co. Ltd.; methanol (HPLC grade) was from Tianjin Siyou Chemicals Co. Ltd.; BT (99%), 3-MT (99%) and DBT (99%) were from J&K Scientific Ltd.; 4,6-DMDBT (99%) was from Beingjing HWRK Chemicals Co. Ltd. All reagents were used as received without further purification.

1.2. Apparatus for characterization

The Fourier Transform Infrared spectra (FT-IR) were tested on a Nicolet FTIR-170SX spectrometer with KBr pellets in the range of 400-4000 cm^{-1}. Powder X-ray diffraction (XRD) was recorded on Rigaku D/max 2500 X-ray diffractometer with scanning rate of 10° min^{-1} and scanning range from 5° to 70°, and incident beam is graphite-monochromatic Cu K_α radiation (λ = 0.15405 nm). Scanning electron microscopy (SEM) and Energy Dispersive Spectrometer (EDS) were performed on a Zeiss Supra55 scanning electron microscopy with an accelerating voltage of 20 kV. Element analysis was measured on ARL9800 X-ray fluorescence spectrometer (XRF). Mechanical strength data were collected using YHKC-2A particle strength tester. TG-DTA were tested on Netzsch STA449 thermogravimetric analyzer with heating rate of 10° min^{-1} from 25 to 800 ºC in the air.

The sulfur contents were analyzed by HPLC Agilent 1100 series with C-18 column, diameter 4.6 mm, length 250 mm, diameter of filler 5 μm, 10% water and 90% methanol as the initial mobile phase, gradient elution to 100% methanol in 10 min with flow rate of 1.0 mL min^{-1}.

1.3. Preparation of adsorbents

1.3.1 Pretreatment of γ-Al_2O_3 beads

The γ-Al_2O_3 beads were washed three times in deionized water, placed in muffle furnace with calcination of 200 ºC for 2 h after drying, getting rid of water molecules and other impurity molecules.

1.3.2 Preparation of adsorbents

MOF-5 was prepared by some modifications in accordance with the literature method.[S1] The detailed procedures are as follows: in a 50 mL of Teflon-lined stainless-steel autoclave, 1.5 mmol of terephthalic acid and 3 mmol zinc nitrate hexahydrate were dissolved in 30 mL DMF, stirring 0.5 h, and then the mixture was heated at 120 ºC for 21 h. After the autoclave cooling to room temperature, the product was separated, washed with DMF (3 × 10 mL), and immersed in chloroform for three days (3 × 10 mL), changing solution every 24 h. The material was then evacuated at 70 ºC for 12 h to remove water molecules and stored in desiccator.

IRMOF-3 was prepared by some modifications in accordance with the literature method.[S2] The detailed procedures are as follows: in a 50 ml of Teflon-lined stainless-steel autoclave, 0.6 mmol of 2-amino terephthalic acid and 1.8 mmol zinc nitrate hexahydrate were dissolved in 30 mL DMF, stirring 0.5 h, and then the mixture was heated at 110 ºC for 48 h. After the autoclave cooling to room temperature, the product was separated, washed with DMF (3 × 10 mL), and immersed in chloroform for three days (3 × 10 mL), changing solution every 24 h. The material was then evacuated at 70 ºC for 12 h to remove water molecules and stored in desiccator.

The preparation methods of MOF-5@γ-Al_2O_3 and IRMOR-3@γ-Al_2O_3 were the same with those of the corresponding MOFs except for introduction of 1.0 g γ-Al_2O_3 beads into the mixed solution of the other reactants, which had been stirred for 0.5 h previously.

1.4. Adsorption desulfurization performance

1.4.1 Preparation of model oil

A certain amount of BT, DBT, 3-MT, 4,6-DMDBT was dissolved in 20 g n-octane solution, and the initial sulfur content of model oil was 1000 $ppmw_S$.

1.4.2 Adsorption desulfurization experiments

Prior to adsorption experiments, γ-Al_2O_3 beads, MOF-5, IRMOF-3 and MOF-5@γ-Al_2O_3, IRMOF-3@γ-Al_2O_3 composite materials were degassed under vacuum at 150 ºC overnight to remove water and other contaminants. Treated adsorbents were added into round bottom flask with model oil in water bath at atmospheric pressure under stirring for 1 h, controlling the temperature of 20, 30, 40 and 50 ºC, respectively. The liquid phase was then separated from the adsorbent by filtration and the S-content of the treated oil was determined by HPLC.

The adsorption capacity under different experimental conditions was calculated by the following formula:

$$Q_i = \frac{W}{M}(C_0 - C_i) \times 10^{-3} \qquad (1)$$

Where Q_i is the adsorption capacity of sulfur adsorbed on the adsorbent (mg $S \cdot g^{-1}$ MOF), W is the mass of model oil (g), M is the mass of the MOF used (g), and C_0 and C_i are the initial and final S-concentrations in the model oil (μg/g), respectively.

1.4.2 Adsorbents regeneration experiment

After adsorption desulfurization experiment, adsorbents were washed in acetone using soxhlet extractor. The eluent samples were analyzed by HPLC, until peaks of sulfur-containing compounds no longer appear, showing sulfur-containing compounds removed completely. After washing, adsorbents were dried under vacuum at 100 ºC for 12 h and experiments for reusing are the same with the as-synthesized samples.

2. Effect of time on the absorption capabilities

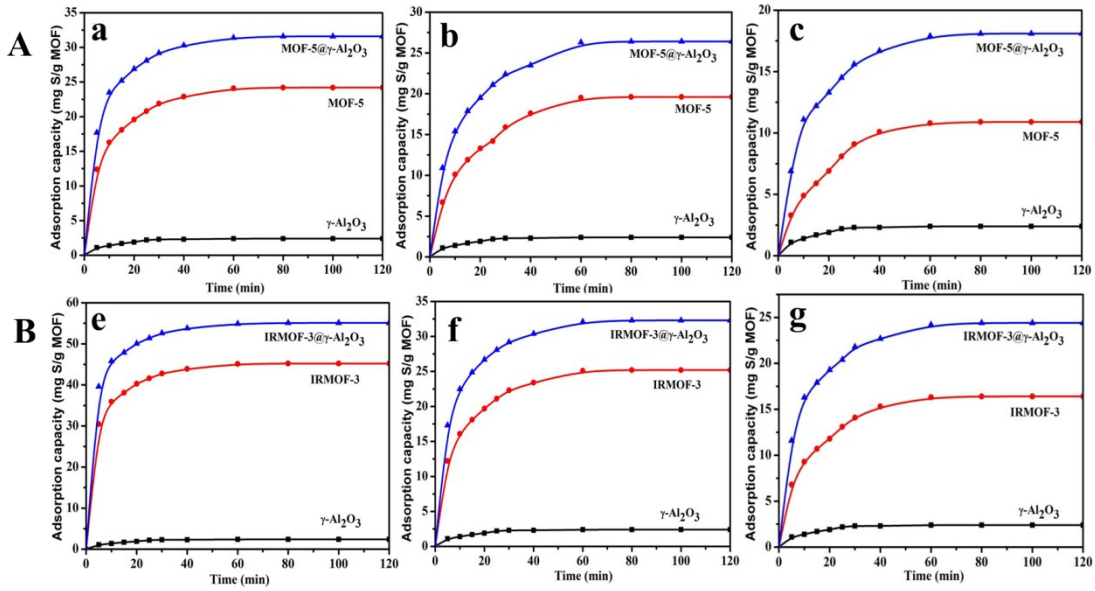

Fig. S1 Effect of adsorption time on desulfurization capacity for DBT (a, e), 3-MT (b, f), 4,6-DMDBT (c, g) over γ-Al_2O_3, MOF-5, MOF-5@γ-Al_2O_3 (A) and γ-Al_2O_3, IRMOF-3, IRMOF-3@γ-Al_2O_3 (B). Conditions: model oil 20 g, γ-Al_2O_3 0.5 g，MOF-5 0.05 g，MOF-5/IRMOF-3@γ-Al_2O_3 0.5 g, [BT], [DBT], [3-MT] and [4,6-DMDBT] 1000 $ppmw_S$, temperature 30 ºC.

Table S1. The adsorption capacities of the obtained MOFs and composites at 10 and 60 min.[a]

	MOF-5	MOF-5@γ-Al_2O_3	IRMOF-3	IRMOF-3@γ-Al_2O_3
Adsorption capacity at 10 min				
BT	21.1	30.6	32.1	40.8
DBT	16.3	23.5	35.9	45.8
3-MT	10.1	19.5	16.1	22.5
DMDBT	4.9	11.1	9.3	16.3
Adsorption capacity at 60 min				
DBT	24.1	31.4	45.1	54.9
3-MT	15.4	26.3	25.1	32.1
DMDBT	10.8	17.9	16.3	24.2
BT	31.9	40.7	41.7	50.6

[a]Reaction conditions: model oil 20 g, γ-Al_2O_3 0.5 g, MOF-5 0.05 g, MOF-5/IRMOF-3@γ-Al_2O_3 0.5 g, [BT], [DBT], [3-MT] and [4,6-DMDBT] 1000 $ppmw_S$, temperature 30 ºC.

3. Effect of temperature on the absorption capabilities

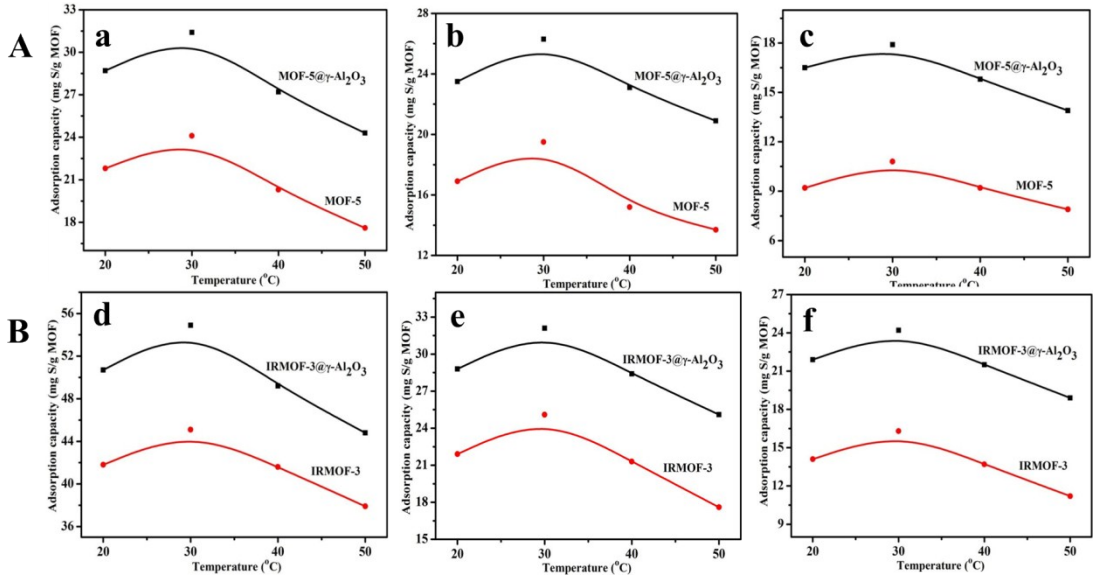

Fig. S2 Effect of adsorption temperature on desulfurization capacity for DBT (a, d), 3-MT (b, e), 4,6-DMDBT (c, f) over γ-Al_2O_3, MOF-5, MOF-5@γ-Al_2O_3 (A) and γ-Al_2O_3, IRMOF-3, IRMOF-3@γ-Al_2O_3 (B). Conditions: model oil 20 g, γ-Al_2O_3 0.5 g，MOF-5 0.05 g，MOF-5/IRMOF-3@γ-Al_2O_3 0.5 g, [BT], [DBT], [3-MT] and [4,6-DMDBT] 1000 $ppmw_S$, time 60 min.

Table S2. The adsorption capacities of the obtained MOFs and composites at 30 ºC.[a]

	MOF-5	MOF-5@γ-Al_2O_3	IRMOF-3	IRMOF-3@γ-Al_2O_3
BT	32.0	40.8	41.6	50.7
DBT	24.1	31.5	45.2	54.9
3-MT	19.6	26.3	25.2	32.0
DMDBT	10.8	18.0	16.4	24.2

[a]Reaction conditions: model oil 20 g, γ-Al_2O_3 0.5 g, MOF-5 0.05 g, MOF-5/IRMOF-3@γ-Al_2O_3 0.5 g, [BT], [DBT], [3-MT] and [4,6-DMDBT] 1000 $ppmw_S$, time 60 min.

4. Effect of mass ratio between oil and adsorbent on absorption capabilities

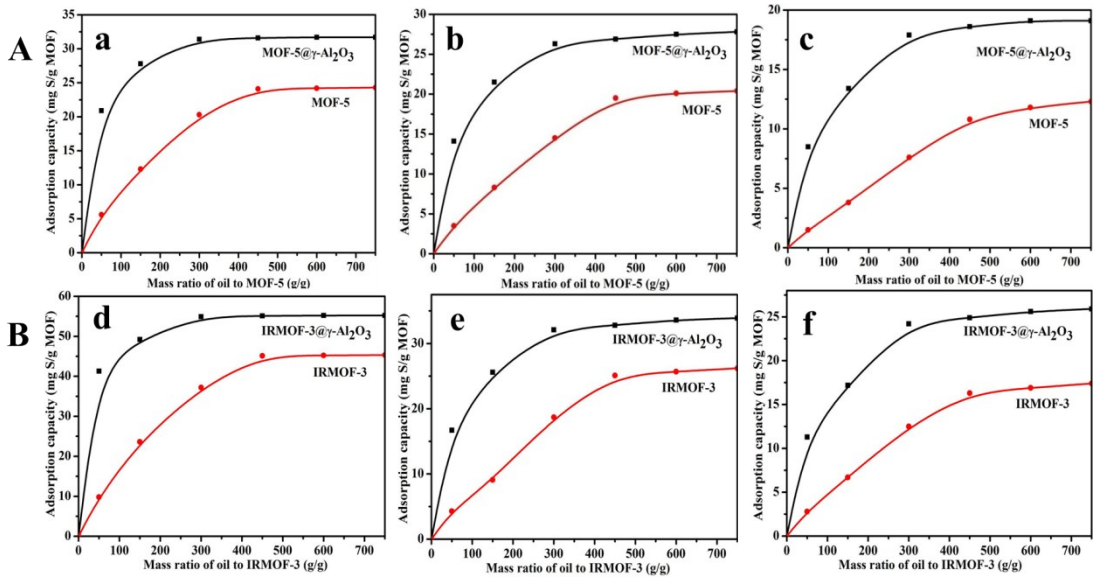

Fig. S3 Effect of mass ratio between oil and adsorbent on desulfurization capacity for DBT (a, d),

3-MT (b, e), 4,6-DMDBT (c, f) over MOF-5, MOF-5@γ-Al_2O_3 (A) and IRMOF-3, IRMOF-3@γ-Al_2O_3 (B). Conditions: model oil 20 g, [BT], [DBT], [3-MT] and [4,6-DMDBT] 1000 $ppmw_S$, temperature 30 ºC, time 60 min.

5. Reusability of the adsorbents

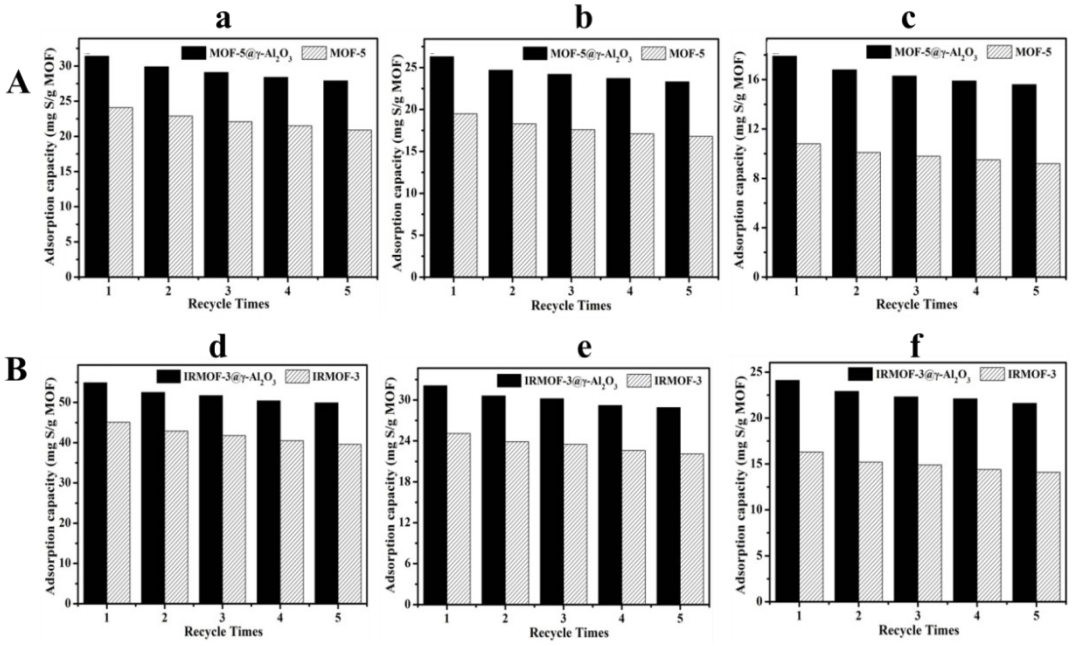

Fig. S4 Effect of recycle times of MOF-5, MOF-5@γ-Al_2O_3 (A) and IRMOF-3 and IRMOF-3@γ-Al_2O_3 (B) on sulfur adsorption capacities for DBT (a), 3-MT (b), DMDBT (c). Conditions: model oil 20g, the mass ratio $M_{MOF\text{-}5@\gamma\text{-}Al_2O_3}/M_{oil}$ 1:40, [BT]、[DBT]、[3-MT]、[4,6-DMDBT] 1000$ppmw_S$, time 60 min, temperature 30 ºC.

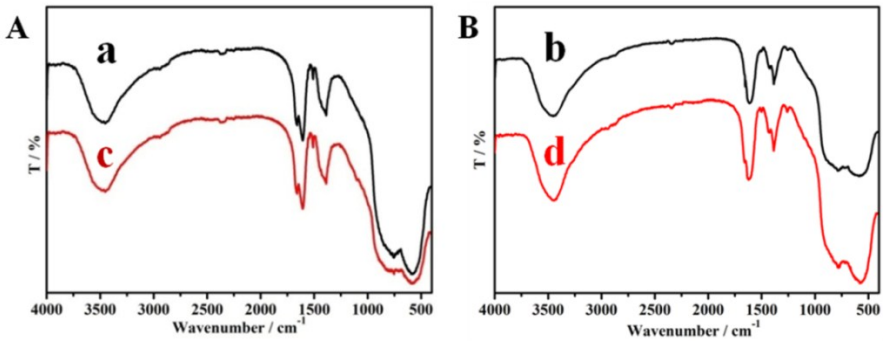

Fig. S5 FT-IR spectra of the fresh (a, b) and fifth regenerated (c, d) of MOF-5@γ-Al_2O_3 (A) and IRMOF-3@γ-Al_2O_3 (B) for BT.

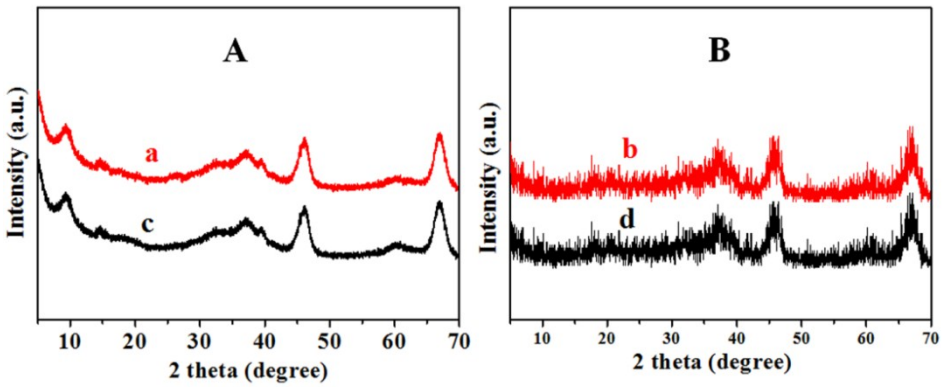

Fig. S6 XRD spectra of the fresh (a, b) and fifth regenerated (c, d) of MOF-5@γ-Al_2O_3 (A) and IRMOF-3@γ-Al_2O_3 (B) for BT.

6. Kinetic analysis

Kinetic constant was calculated by second-order kinetic equations as follows:[S3, S4]

$$\frac{t}{q_t} = \frac{1}{k_2 q_e^2} + \frac{1}{q_e} t \qquad (2)$$

where q_e is equilibrium adsorption capacity (mg S/g MOF), q_t is adsorption capacity at time t (mg S/g MOF), k_2 is second-order kinetic equilibrium constant.

The pseudo-second order kinetics of BT adsorption over the MOFs

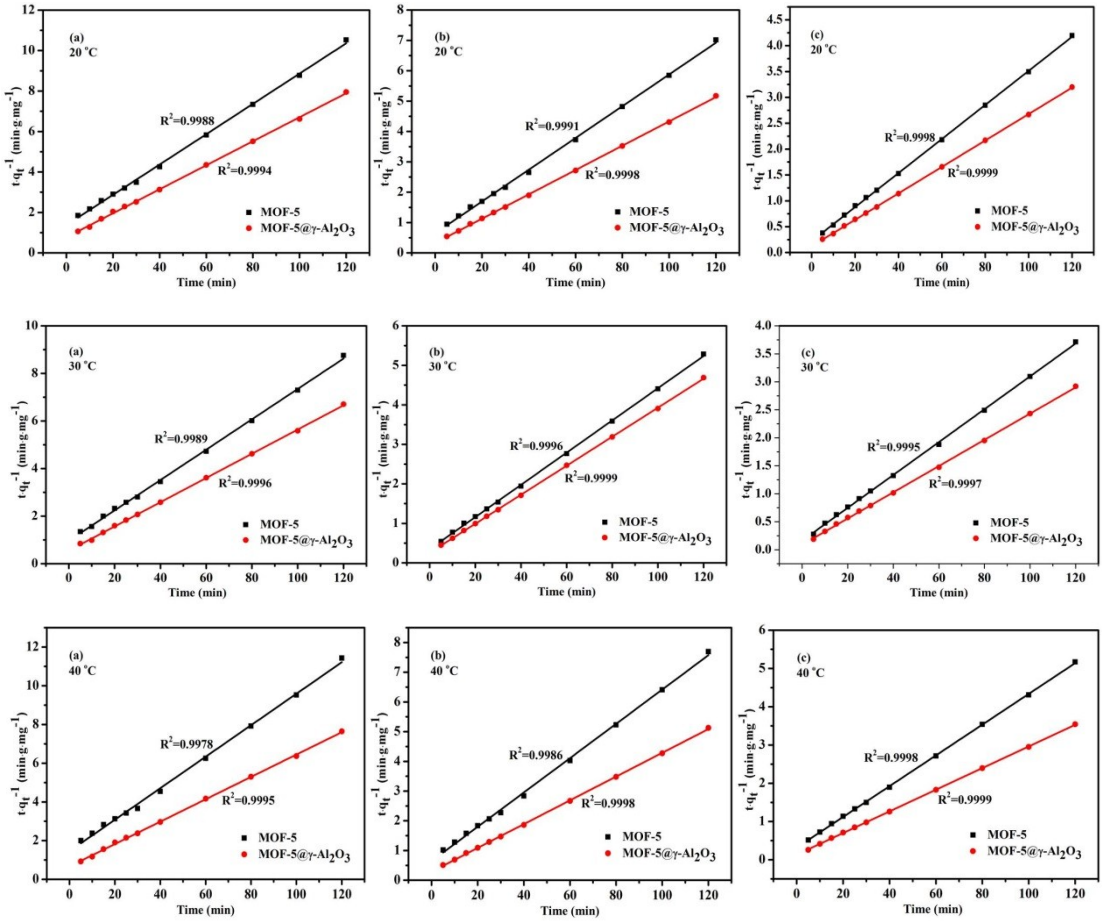

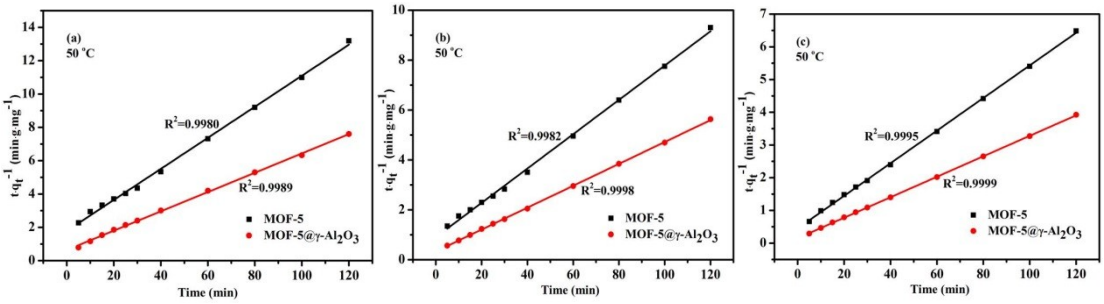

Fig. S7 Plots of pseudo-second order kinetics of BT adsorption over MOF-5 and MOF-5@γ-Al_2O_3 at different temperature: C_0 = 250 (a), 500 (b) and 1000 (c) $ppmw_S$.

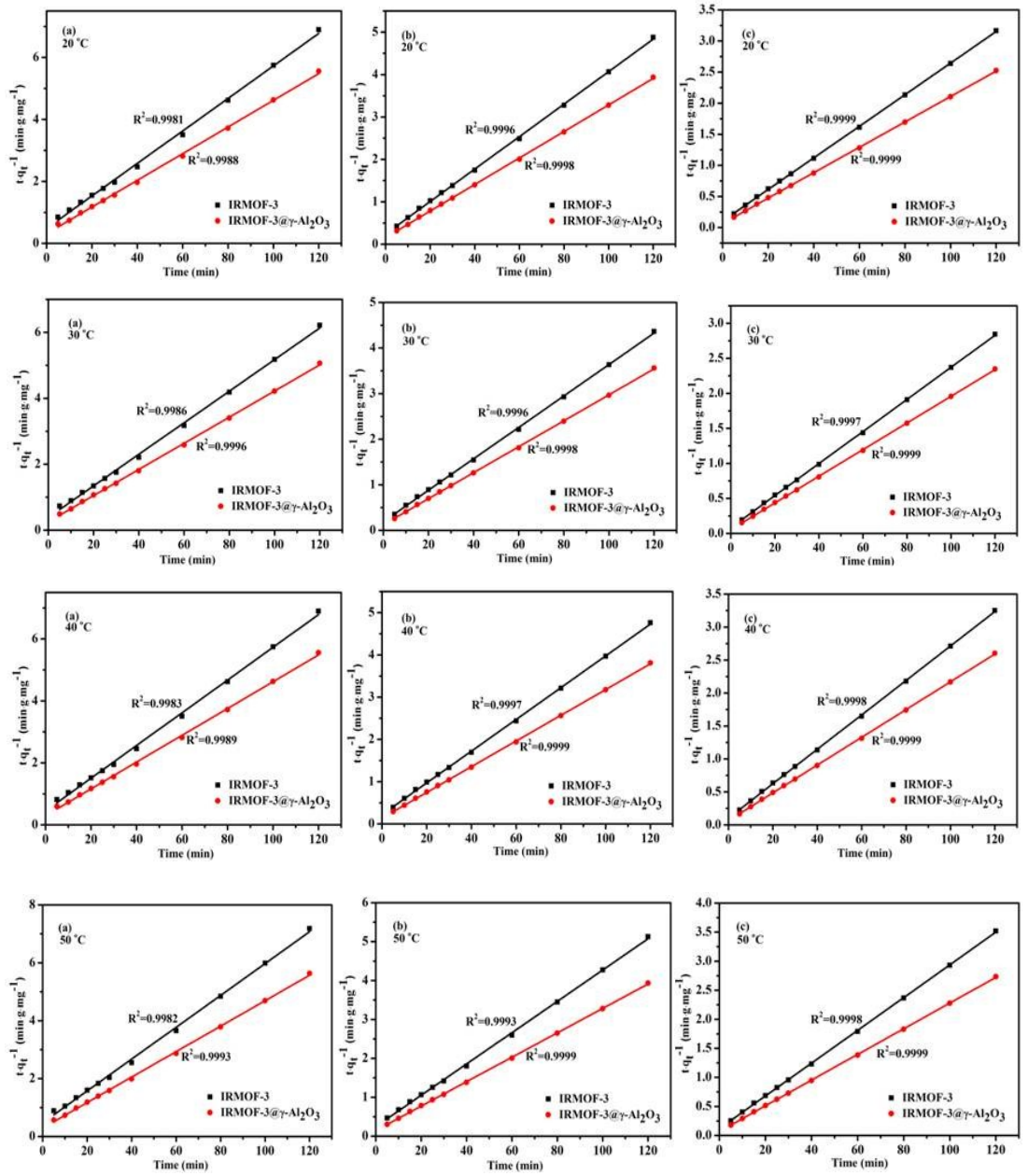

Fig. S8 Plots of pseudo-second order kinetics of BT adsorption over IRMOF-3 and IRMOF-3@γ-Al_2O_3 at different temperature: C_0 = 250 (a), 500 (b) and 1000 (c) $ppmw_S$.

Table S3. The pseudo-second-order kinetic constants (k_2) of MOF-5、MOF-5@γ-Al_2O_3 and IRMOF-3、IRMOF-3@γ-Al_2O_3 at various DBT concentrations and different temperatures. The maximum adsorption capacities (Q_0) and the molar ratios of DBT that adsorbed on each metal ion are also presented.

Adsorbent	T/°C	k_2/10^{-3} g min^{-1} mg^{-1}			Q_0/mg S g^{-1} MOF	DBT/metal (mol/mol)
		250 ppmw$_S$	500 ppmw$_S$	1000 ppmw$_S$		
MOF-5@ γ-Al_2O_3 (MOF-5)	20	5.07 (4.82)	5.45 (5.05)	5.62 (5.36)	47.68 (35.97)	0.29 (0.22)
	30	5.27 (4.94)	5.59 (5.11)	5.81 (5.65)	50.68 (39.21)	0.31 (0.24)
	40	5.54 (5.19)	5.84 (5.26)	6.13 (5.86)	42.73 (32.28)	0.26 (0.19)
	50	5.71 (5.36)	6.11 (5.51)	6.39 (5.97)	37.57 (27.31)	0.23 (0.16)
IRMOF-3 @γ-Al_2O_3 (IRMOF-3)	20	6.12 (5.89)	6.47 (6.23)	6.71 (6.50)	82.64 (68.49)	0.53 (0.44)
	30	6.33 (6.07)	6.57 (6.35)	6.91 (6.68)	86.58 (72.25)	0.56 (0.46)
	40	6.54 (6.39)	6.79 (6.69)	7.19 (7.04)	74.02 (64.59)	0.47 (0.41)
	50	6.87 (6.64)	6.97 (6.86)	7.29 (7.12)	65.74 (57.21)	0.42 (0.37)

Table S4. The pseudo-second-order kinetic constants (k_2) of MOF-5、MOF-5@γ-Al_2O_3 and IRMOF-3、IRMOF-3@γ-Al_2O_3 at various 3-MT concentrations and different temperatures. The maximum adsorption capacities (Q_0) and the molar ratios of 3-MT that adsorbed on each metal ion are also presented.

Adsorbent	T/°C	k_2/10^{-3} g min^{-1} mg^{-1}			Q_0/mg S g^{-1} MOF	3-MT/metal (mol/mol)
		250 ppmw$_S$	500 ppmw$_S$	1000 ppmw$_S$		
MOF-5@ γ-Al_2O_3 (MOF-5)	20	3.21 (2.89)	3.49 (2.97)	3.58 (3.05)	29.76 (21.82)	0.18 (0.13)
	30	3.31 (2.94)	3.54 (3.11)	3.62 (3.37)	32.65 (24.73)	0.19 (0.15)
	40	3.41 (3.19)	3.60 (3.39)	3.91 (3.59)	28.44 (19.01)	0.17 (0.11)
	50	3.57 (3.31)	3.76 (3.57)	3.99 (3.64)	25.24 (16.91)	0.15 (0.11)
IRMOF-3 @γ-Al_2O_3 (IRMOF-3)	20	3.97 (3.57)	4.16 (3.89)	4.56 (4.17)	35.99 (27.89)	0.23 (0.17)
	30	4.26 (3.87)	4.62 (4.21)	5.09 (4.77)	39.15 (31.26)	0.25 (0.19)
	40	4.33 (4.02)	4.77 (4.42)	5.19 (4.96)	34.09 (26.13)	0.21 (0.16)
	50	4.93 (4.26)	5.08 (4.73)	5.43 (5.29)	29.94 (21.31)	0.19 (0.14)

Table S5. The pseudo-second-order kinetic constants (k_2) of MOF-5、MOF-5@γ-Al_2O_3 and IRMOF-3、IRMOF-3@γ-Al_2O_3 at various 4,6-DMDBT concentrations and different temperatures. The maximum adsorption capacities (Q_0) and the molar ratios of 4,6-DMDBT that adsorbed on each metal ion are also presented.

Adsorbent	T/°C	k_2/10^{-3} g min^{-1} mg^{-1}			Q_0/mg S g^{-1} MOF	4,6-DMDBT/metal (mol/mol)
		250 ppmw$_S$	500 ppmw$_S$	1000 ppmw$_S$		
MOF-5@ γ-Al_2O_3 (MOF-5)	20	4.07 (3.45)	4.32 (3.83)	4.56 (4.14)	18.84 (11.21)	0.11 (0.07)
	30	4.44 (4.11)	4.87 (4.42)	5.07 (4.74)	20.21 (12.81)	0.12 (0.08)
	40	4.75 (4.28)	5.24 (4.56)	5.54 (5.01)	17.65 (10.84)	0.11 (0.06)

IRMOF-3 @γ-Al_2O_3 (IRMOF-3)	**50**	5.17 (4.79)	5.45 (5.17)	5.63 (5.32)	15.39 (9.18)	0.09 (0.05)
	20	4.45 (4.18)	4.87 (4.58)	5.06 (4.83)	24.79 (16.48)	0.16 (0.11)
	30	4.56 (4.44)	5.01 (4.82)	5.38 (5.15)	27.01 (18.95)	0.17 (0.12)
	40	5.15 (4.75)	5.32 (5.01)	5.78 (5.31)	24.16 (15.91)	0.15 (0.10)
	50	5.26 (4.91)	5.59 (5.25)	6.01 (5.78)	21.46 (12.87)	0.13 (0.08)

7. Thermodynamic analysis

Adsorption isotherm was simulated by Langmuir adsorption isothermal model with the Langmuir equation as follows:[34,36]

$$\frac{C_e}{q_e} = \frac{C_e}{Q_0} + \frac{1}{Q_0 b} \qquad (3)$$

where C_e is equilibrium concentration of the sulfur in model oil (mg/L), q_e is equilibrium adsorption capacity (mg S/g MOF), Q_0 is saturated adsorption capacity (mg S/g MOF), b is Langmuir constant(L/mg). Q_0 and b were deduced by plotting C_e versus C_e/q_e.

To shed light on the thermodynamics of adsorption process, we calculated the Gibbs free energy change (ΔG), enthalpy change (ΔH) and entropy change (ΔS) based on the Gibbs and Van't Hoff equations:[37]

$$\Delta G = -RT\ln b \qquad (4)$$

$$\ln b = \frac{\Delta S}{R} - \frac{\Delta H}{RT} \qquad (5)$$

where b is Langmuir constant (L/mol), and enthalpy change (ΔH) and entropy change (ΔS) were determined by plotting ln$b$ versus 1/T.

7.1 Adsorption isotherms of BT over the MOFs

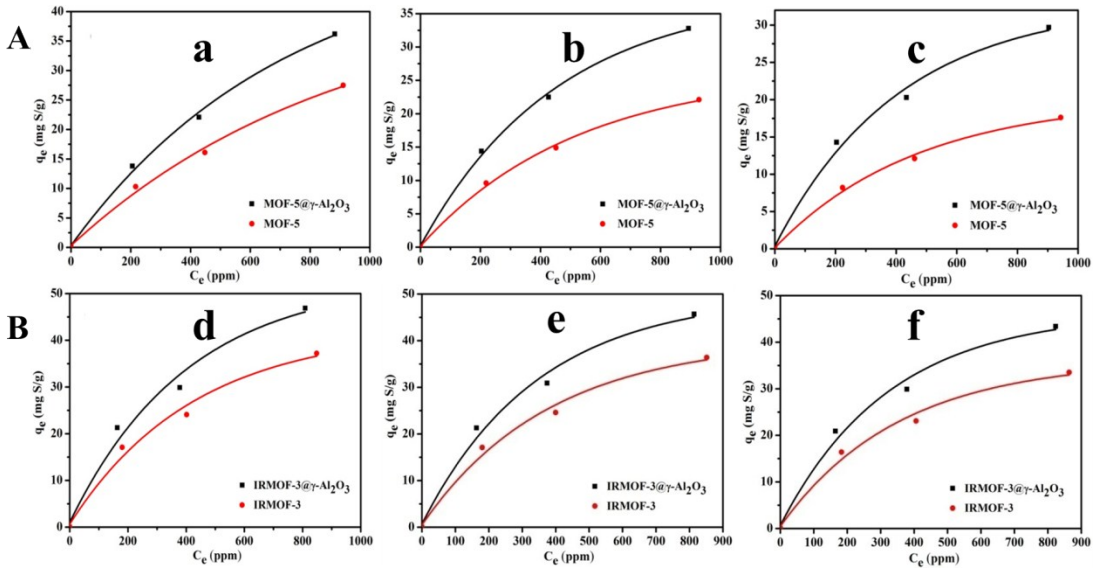

Fig. S9 Adsorption isotherms of BT over MOF-5 and MOF-5@γ-Al_2O_3 (A), IRMOF-3 and IRMOF-3@γ-Al_2O_3 (B) at 20 ºC (a, d), 40 ºC (b, e) and 50 ºC (c, f).

7.2 The Langmuir fitting curves for SCCs over the adsorbents

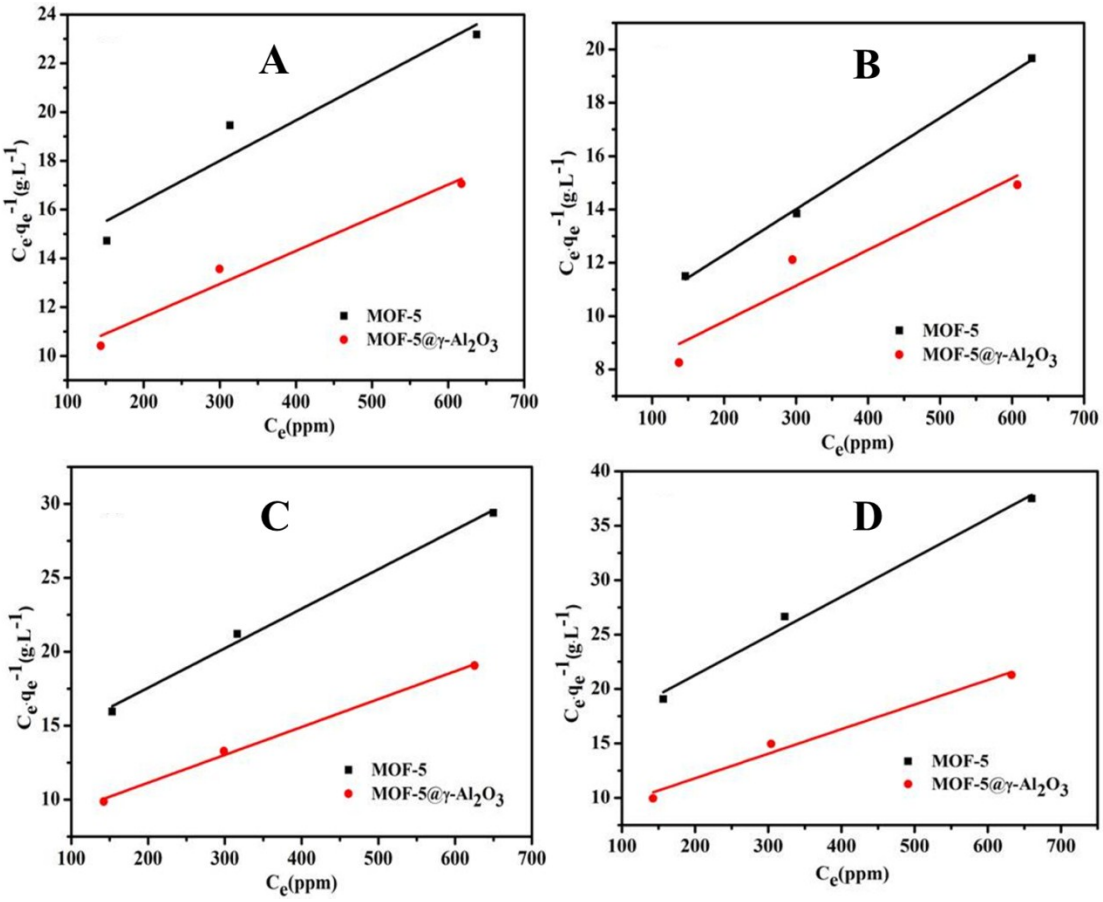

Fig. S10 Langmuir fitting curves for BT over MOF-5 and MOF-5@γ-Al_2O_3 at 20 ºC (A), 30 ºC (B), 40 ºC (C) and 50 ºC (D).

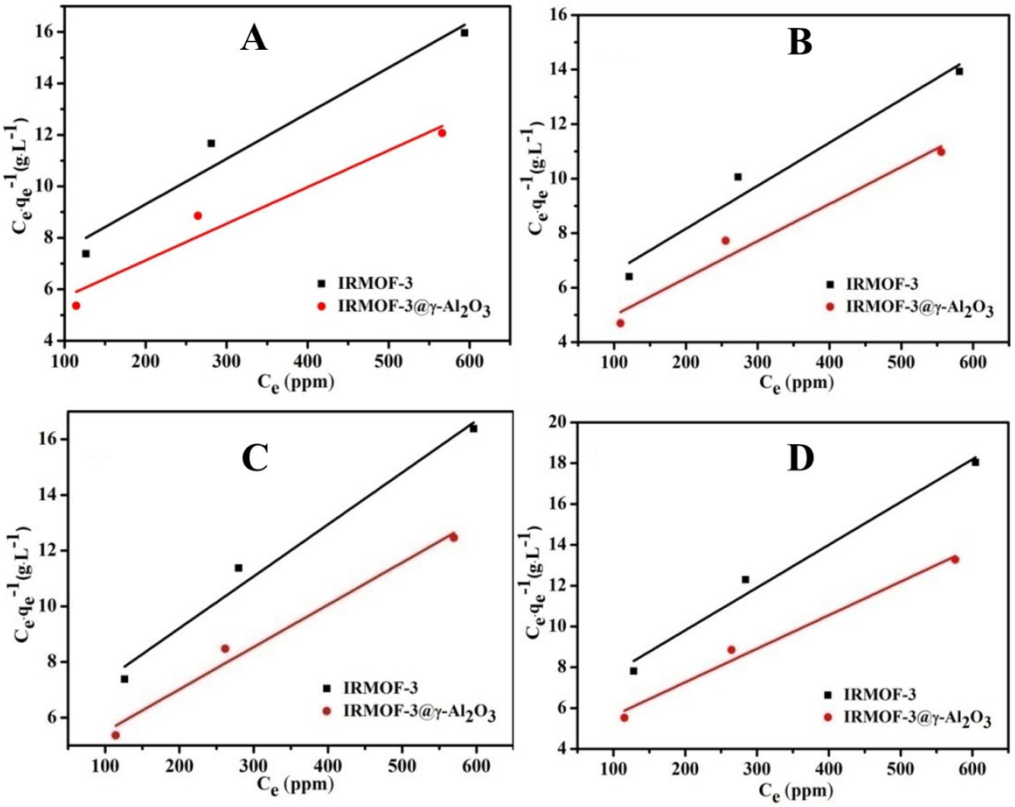

Fig. S11 Langmuir fitting curves for BT over IRMOF-3 and IRMOF-3@γ-Al_2O_3 at 20 ºC (A), 30 ºC (B), 40 ºC (C) and 50 ºC (D).

7.3 . Plots of Inb versus 1/T for the adsorbents

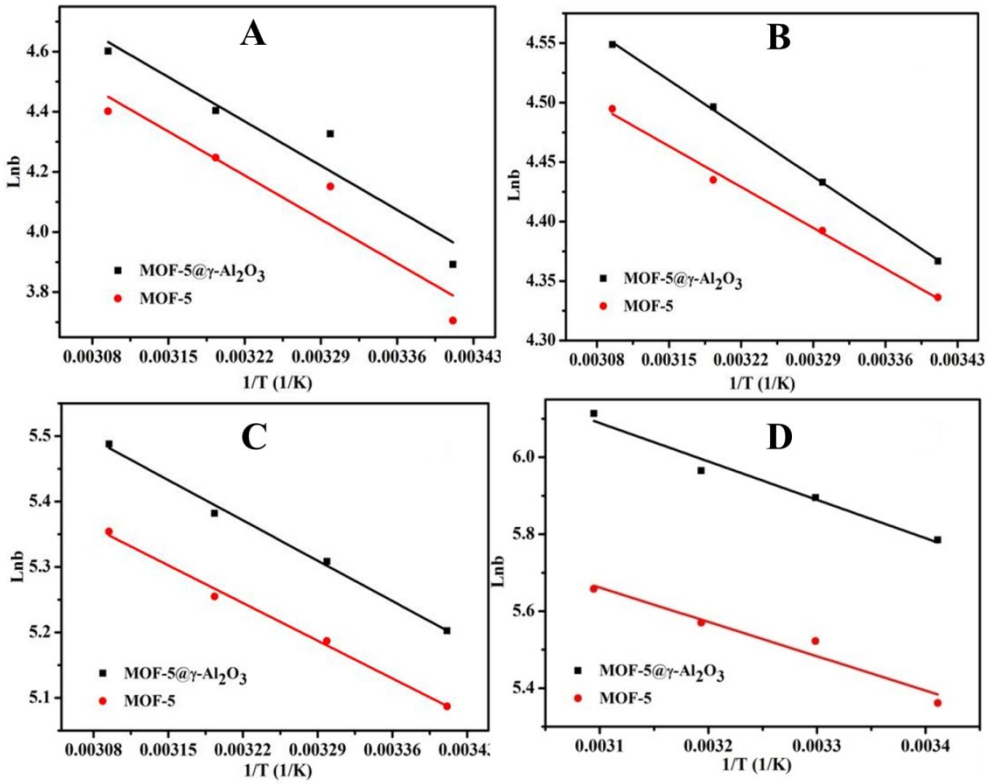

Fig. S12 Plots of ln*b* versus 1/T of MOF-5 and MOF-5@γ-Al_2O_3: BT (A), DBT (B), 3-MT (C), 4,6-DMDBT (D).

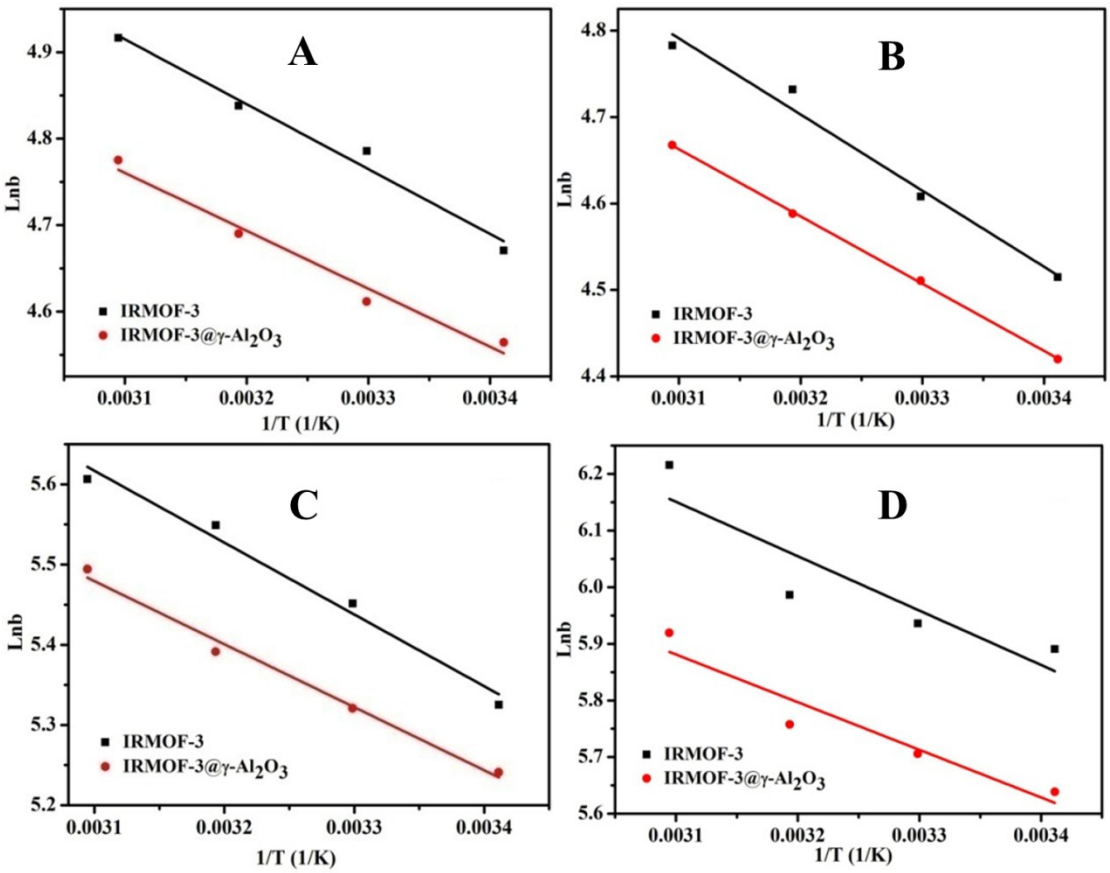

Fig. S13 Plots of ln*b* versus 1/T of IRMOF-3 and IRMOF-3@γ-Al_2O_3: BT (A), DBT (B), 3-MT (C), 4,6-DMDBT (D).

Table S6. The thermodynamic parameters of DBT adsorption over MOF-5@γ-Al_2O_3 and IRMOF-3@γ-Al_2O_3 at different temperatures.

Adsorbent	T/°C	Δ*G*/ kJ mol^{-1}	Δ*H*/kJ mol^{-1}	Δ*S*/J mol^{-1} K^{-1}
MOF-5@γ-Al_2O_3 (MOF-5)	20	-10.64 (-10.57)	4.81 (4.08)	52.72 (49.96)
	30	-11.17 (-11.07)		
	40	-11.71 (-11.54)		
	50	-12.21 (-12.08)		
IRMOF-3@γ-Al_2O_3 (IRMOF-3)	20	-11.37 (-10.85)	7.44 (6.53)	69.76 (65.81)
	30	-11.84 (-11.44)		
	40	-12.32 (-11.95)		
	50	-12.85 (-12.54)		

Table S7. The thermodynamic parameters of 3-MT adsorption over MOF-5@γ-Al_2O_3 and IRMOF-3@γ-Al_2O_3 at different temperatures.

Adsorbent	T/°C	Δ*G*/ kJ mol^{-1}	Δ*H*/kJ mol^{-1}	Δ*S*/J mol^{-1} K^{-1}

MOF-5@γ-Al_2O_3 (MOF-5)	20	-12.68 (-12.39)	6.57 (6.06)	67.04 (64.26)
	30	-13.37 (-13.06)		
	40	-14.01 (-13.68)		
	50	-14.74 (-14.38)		
IRMOF-3@γ-Al_2O_3 (IRMOF-3)	20	-12.98 (-12.77)	7.32 (6.84)	68.23 (65.64)
	30	-13.74 (-13.41)		
	40	-14.45 (-14.04)		
	50	-15.06 (-14.76)		

Table S8. The thermodynamic parameters of 4,6-DMDBT adsorption over MOF-5@γ-Al_2O_3 and IRMOF-3@γ-Al_2O_3 at different temperatures.

Adsorbent	**T/ºC**	**Δ*G*/kJ mol^{-1}**	**Δ*H*/kJ mol^{-1}**	**Δ*S*/J mol^{-1} K^{-1}**
MOF-5@γ-Al_2O_3 (MOF-5)	20	-14.11 (-13.07)	7.98 (6.99)	75.89 (70.06)
	30	-14.86 (-13.92)		
	40	-15.53 (-14.51)		
	50	-16.43 (-15.20)		
IRMOF-3@γ-Al_2O_3(IRMOF-3)	20	-14.36 (-13.74)	8.29 (7.41)	76.33 (70.58)
	30	-15.31 (14.38)		
	40	-15.59 (-14.83)		
	50	-15.86 (-15.41)		

References

S1. J. Hafizovic, M. Bjørgen, U. Olsbye, P. D. C. Dietzel, S. Bordiga, C. Prestipino, C. Lamberti and K. P. Lillerud, J. Am. Chem. Soc., 2007, 129, 3612-3620.

S2. X.-L. Wang, H.-L. Fan, Z. Tian, E.-Y. He, Y. Li and J. Shangguan, Appl. Surf. Sci., 2014, 289, 107-113.

S3. Y. S. Ho and G. McKay, Process Biochem., 1999, 34, 451-465.

S4. B. H. Hameed and A. A. Rahman, J. Hazard. Mater., 2008, 160, 576-581.